# Ultrafast Charge Transfer at Monolayer Graphene Surfaces with Varied Substrate Coupling

Silvano Lizzit,[†] Rosanna Larciprete,[‡] Paolo Lacovig,[†] Krassimir L. Kostov,[§] and Dietrich Menzel[⊥],[*]

[†]Elettra-Sincrotrone Trieste S.C.p.A., S.S. 14 Km 163.5, 34149 Trieste, Italy, [‡]CNR—Institute for Complex Systems, Via Fosso del Cavaliere 100, 00133 Roma, Italy, [§]Institute of General and Inorganic Chemistry, Bulgarian Academy of Sciences, 1113 Sofia, Bulgaria, and [⊥]Physik-Department E20, Technische Universität München, 85748 Garching, Germany, and Fritz-Haber-Institut der MPG, Department CP, 14195 Berlin, Germany

ABSTRACT The charge transfer rates of a localized excited electron to graphene monolayers with variable substrate coupling have been investigated by the core hole clock method with adsorbed argon. Expressed as charge transfer times, we find strong variations between ∼3 fs (on graphene "valleys" on Ru(0001)) to ∼16 fs (quasi-free graphene on SiC, O/Ru(0001), or SiO_2/Ru). The values for the "hills" on Gr/Ru and on Gr/Pt(111) are in between, with the ratio 1.7 between the charge transfer times measured on "hills" and "valleys" of Gr/Ru. We discuss the results for Gr on metals in terms of

hybridized Ru—C orbitals, which change with the relative Gr—Ru alignment and distance. The charge transfer on the decoupled graphene layers must represent the intrinsic coupling to the graphene empty π^* states. Its low rate may be influenced by processes retarding the spreading of charge after transfer.
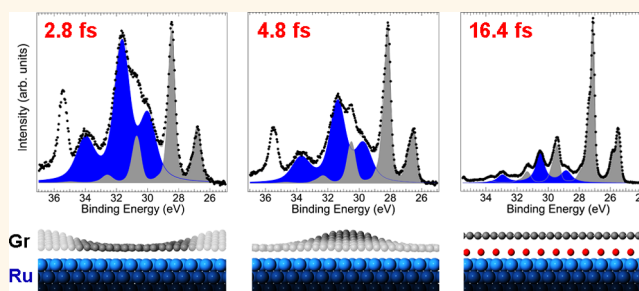
KEYWORDS: epitaxial graphene · charge transfer · Auger resonant Raman · argon · oxygen intercalation · Ru(0001) · Pt(111) · SiC(0001) · SiO_2

The exciting properties of graphene[1] are being vigorously investigated with the full arsenal of available experimental and theoretical methods. While these studies provide a wealth of information on the electronic, chemical, and structural properties of graphene (Gr), many aspects are still unclear or controversial. In particular, little is known about the dynamics of charge transfer (CT) of adsorbed species on Gr. The CT between adsorbates and surfaces is important for the electronic response of surfaces and for photochemistry on surfaces.[2] On metals and semiconductors the corresponding times for weak to medium adsorbate coupling lie in the low femtosecond range, and for strong coupling they can be in the sub-femtosecond range.[3,4] These very short CT times are the basis of the strong substrate influence on electronically induced reactions at metal and semiconductor surfaces; they have long been deduced indirectly from these observations.[2] One possibility to directly measure

them is the so-called core hole clock (CHC) method,[5,6] in which the transfer time of an excited electron localized on an adsorbate (created by a resonant core hole excitation of that atom) to the substrate is determined by a quantitative analysis of the corresponding core hole decay spectra.

In this method an adsorbate core electron is resonantly excited to a bound empty state of that atom by absorption of a narrow-band photon, creating an excited electron atomically localized at a defined position in front of the surface. This electron can be transferred to the substrate if its wave function overlaps with an empty state wave function of the surface. The core hole decay electron spectra differ for the cases in which this transfer happens before or after the refilling of the core hole by Auger decay. For core hole decay before CT the locally excited electron is still locally present at the instance of decay, so that two-hole one-electron states or one-hole states (energetically equivalent to satellite and main lines in

direct photoemission) of the adatom result; the corresponding spectra are usually called resonant photoemission or resonant Auger Raman spectra. For CT before core hole decay two-hole decay (Auger) spectra result. These two types of spectra can be disentangled by the shifts of peaks upon tuning the photon energy through the resonance: for the first type the decay electrons have constant binding energy, the second constant kinetic energy. More detailed analysis shows that the first type of excitation/decay is a coherent one-step process and the second one an incoherent two-step process.[7] The charge transfer time, τ_{CT}, is determined from the intensity ratio of the integrated Raman and Auger spectra, (I_R) and (I_A), multiplied by the core hole decay time, τ_H. In this way τ_H is used as an internal clock ticking at some femtoseconds. Depending on data quality a range of about 1/10 to 10 times the τ_H is accessible.[6] A very convenient probe atom is physisorbed Ar, because its Ar $2p_{3/2} \rightarrow 4s$ excitation is accessible with narrow bandwidth, and its decay spectra can be obtained with high resolution and disentangled into coherent Raman and incoherent Auger contributions with good precision using the shifts occurring when detuning the exciting photon energy through the resonance. The weak surface bond of Ar and the consequent weak coupling lead to CT times in the low femtosecond range, which compare well with the Ar 2p core hole lifetime of about 6 fs.

On metal surfaces τ_{CT} has been shown[8,9] to depend mainly on the overlap of the excited electron's orbital with empty surface states of proper energy and symmetry. Connections exist to the tunnelling probability seen in scanning tunnelling microscopy (STM) at certain bias voltages and to conduction through atomic chains and molecular bridges. While it may be expected that the main contribution to τ_{CT} of an initially localized excited electron above the surface comes from the transfer to the first neighbor(s), which is/are normally embedded in the surface of a three-dimensional conductor, it cannot be safely assumed that this is always the case, in particular if the recipient of the charge has lower dimensionality. To learn more about the physics of these processes and to obtain information about electron dynamics on Gr, in particular about charge transfer to Gr and charge spreading in it, it appeared very interesting to apply this method to differently coupled graphene monolayers (Gr ML).

Gr ML can be produced on many substrates,[10] showing a wide variation of graded substrate coupling, from very strong—for instance on Ru(0001), which, together with the lattice mismatch, leads to regularly buckled layers[11]—via weak coupling as on Ir(111) or Pt(111),[10] to flat, essentially decoupled layers on SiC,[12−14] on oxygen-dosed Ru(0001),[15] or on thin SiO$_2$ layers on Ru.[16] In all these situations it should be expected that, if the spreading of charge after the initial delocalization has an influence on the overall τ_{CT}, then CT should be faster for Gr coupled to metals than on decoupled Gr; roughly this can be seen as three-dimensional (3D) vs two-dimensional (2D) final states of CT, although the situations may be more complex. Also, the contrast seen in STM of Gr on metal surfaces, and controversially discussed in terms of geometric and electronic contributions to tunnelling in the Ru case,[11,17] should be paralleled by different CT times from the CHC method as well.

Here we show that the dynamics of charge transfer from resonantly excited adsorbed Ar atoms to Gr indeed depends strongly on the coupling of the Gr to its substrate. For decoupled Gr, independent of the way of decoupling, remarkably slow charge transfer (corresponding to $\tau_{CT} \approx 16$ fs) is found. For strong substrate coupling—Gr on Ru—the CT rate is very high (τ_{CT} down to ∼2.5 fs) and is distinctly different for the different positions in the periodically buckled layer, being much faster where Gr is strongly interacting with the metal than in the regions of weak interaction. However, even in the latter regions CT is more than 3 times faster than for decoupled Gr, showing that the metal influences the CT over the entire surface, albeit in a graded way. On Gr/Pt(111) it is even slower. We argue that this graded CT rate can be used for conclusions about the coupling of Gr and the metal substrate. Since CT is then determined by the overlap of the excited electron's orbital with empty density of Ru−C hybridized states above the Gr surface, we interpret these findings by Gr−Ru hybridized states so that metal states effectively reach through the Gr ML, leading to 3D charge spreading. On the other hand, the slow CT on decoupled Gr must be due to more complex effects, which slow it down, as will be discussed.

EXPERIMENTAL RESULTS

The Ar mono- or submonolayers on the various Gr surfaces have been characterized by XAS and XPS (referenced to E_F). The peaks for our various conditions are shown in Figure 1. The exact energy values are compiled in Table 1.

In order to separately record the spectral contributions of the Ar adsorbed in the valleys (L regions) and on the hills (H regions) of Gr/Ru(0001), we have utilized the finding of Brugger et al.[18] that Xe adsorbed on the corrugated surface has slightly higher adsorption energy on L than on H regions, so that a partly (<60%) covered surface contains Xe only in L regions. After verifying that, as expected, the same is the case for adsorbed Ar, we have produced Ar in L only by covering about 50% of the corrugated Gr/Ru surface with Ar. Ar on H regions only was prepared by blocking the L regions with Xe and then adsorbing Ar on H. The XPS data shown in Figure 2 verify this.

The sets of decay spectra obtained tuning the photon energy through the Ar resonance and analyzed as described in Methods comprise the main results. An example for such a data set is shown in Figure 3 for
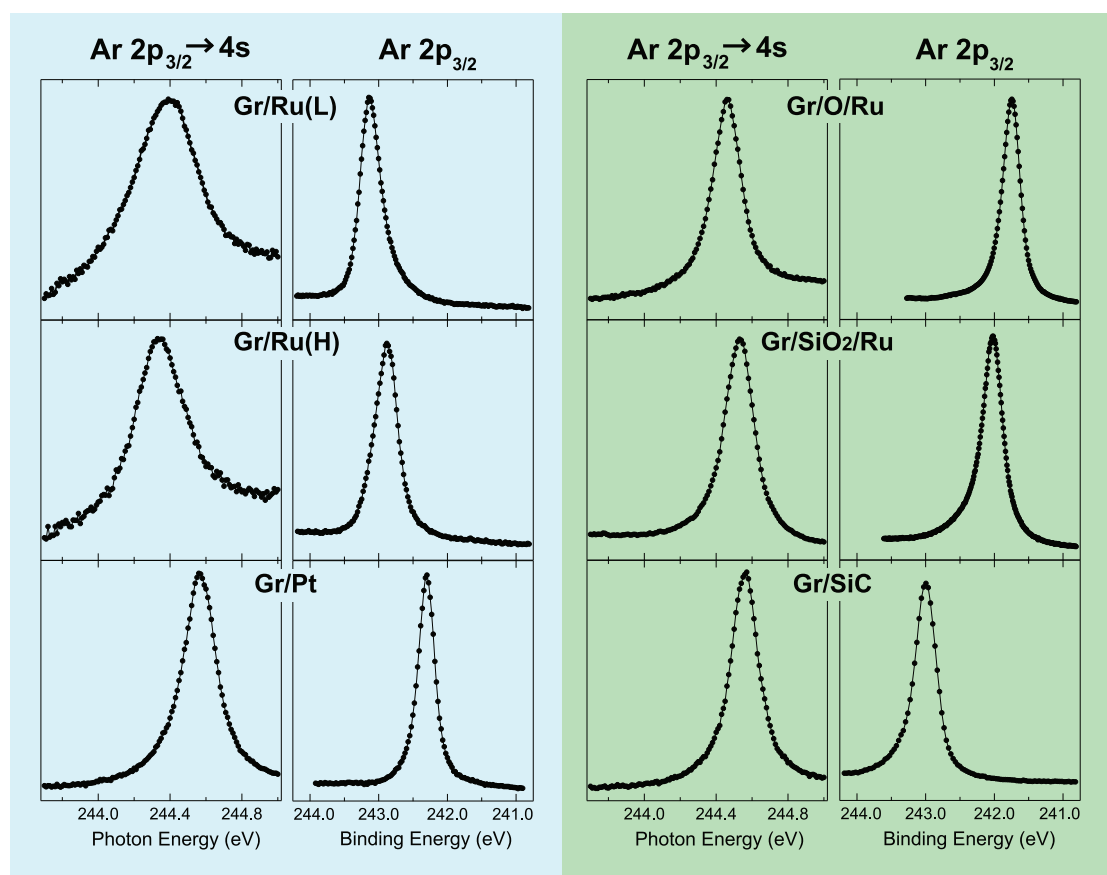
Figure 1. XAS (Ar 2p$_{3/2}$→4s) and XPS (Ar 2p$_{3/2}$) peaks for the various investigated situations. In the green panel are shown the three decoupled cases. For quantitative values see Table 1.

TABLE 1. Compilation of Energies (in eV) and τ_{CT} (in fs) for the Various Conditions Investigated

	XAS Ar^{c+}4s	XPS Ar 2p$_{3/2}$	Ar^{c+} 4s (rel E_F)	τ_{CT}
gas	244.39			
Ru	244.68	241.47	3.21	1.4
Gr/Ru-L	244.40	243.16	1.24	2.8
Gr/Ru-H	244.34	242.86	1.48	4.8
Pt	244.64	240.89	3.75	3.5
Gr/Pt	244.56	242.30	2.26	7.4
Gr/O/Ru	244.46	241.74	2.72	16.4
Gr/SiO$_2$/Ru	244.53	242.02	2.51	16.6
Gr/SiC	244.56	243.00	1.56	16.2

the Gr/Pt(111) case. Figure 4 compiles decay spectra at the resonance maximum and their decomposition into Raman and Auger contributions for four characteristic cases.

Already without any analysis these decay spectra show the strong differences of branching for the various layers: Auger decay predominates for Gr/Ru (L and H), while Raman decay predominates for quasi-decoupled Gr layers (only Gr/O/Ru is shown in the figure; the others—Gr on SiC and on SiO$_2$/Ru—are very

similar). On Pt the two contributions are comparable, as already shown in Figure 3. These differences are borne out by careful analysis of the complete sets (see Methods); Table 1 compiles the quantitative results. To put this into perspective, we also give the CT times for Ar on the clean Ru and Pt surfaces (*i.e.*, without Gr) obtained in the same setup and experimental run; they agree acceptably with older work.[19,20]

DISCUSSION
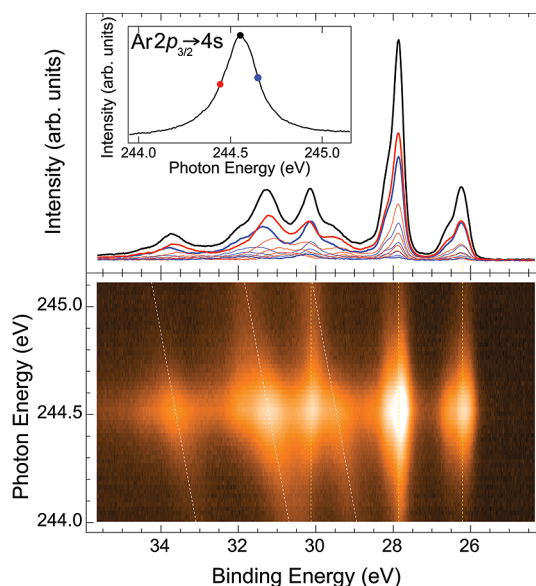
The main results are seen to be as follows:

- Generally, the CT times are quite short (in the low femtosecond regime) and span a considerable range.
- The CT times on the quasi-lifted off layers, Gr/SiC, Gr/O/Ru, and Gr/SiO$_2$, are about the same and much longer, about 6 times longer than on Gr(L)/Ru.
- CT for the hills (H) and the valleys (L) of the corrugated layer on Ru differ clearly: in L the CT is 1.7 times faster than on H.
- On the weakly coupled Gr on Pt(111) τ_{CT} is about halfway between the extremes.
- However, τ_{CT} on Gr hills on Ru and even on Gr/Pt is much shorter than on the quasi-lifted off Gr layers.
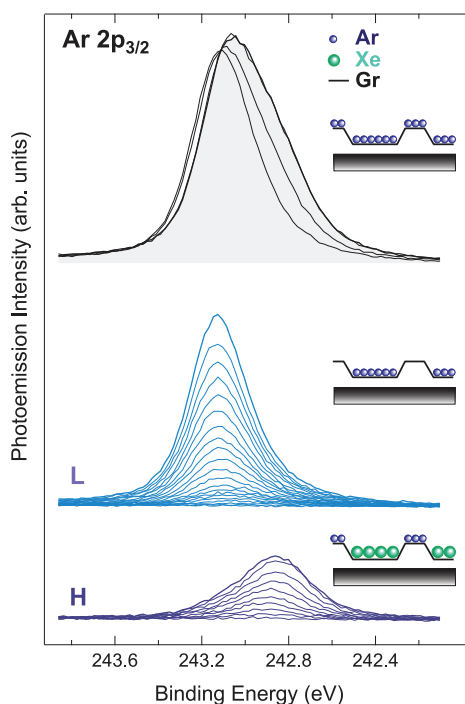
Figure 2. Verification of the method of separately preparing Ar layers on the L and H regions of corrugated Gr/Ru(0001) by XPS of Ar $2p_{3/2}$: Top: The Ar peak as a function of coverage (thin lines) shows that two components are contained. After producing either Ar on L (center) or on H (bottom) as described in the text, the single homogeneous components shown are obtained, which do not shift with coverage. Summing the L and H peaks (each at their maximum coverage) leads to a peak that coincides with the undifferentiated full coverage (top, fat line). This verifies that the individual partial coverages are present in the full layer.

Figure 3. Decay spectra of the resonantly excited $2p_{3/2} \rightarrow 4s$ state of Ar adsorbed on Gr/Pt(111), which allow distinguishing the two decay channels (core hole decay before or after CT) from the peak behavior with photon energy. Top: Some selected decay spectra measured every 100 meV from the complete set of raw data (i.e., containing background, which is seen to be very low) taken every 20 meV through the resonance. Red spectra are below resonance, while blue spectra are above. The black curve represents the decay spectrum on resonance. Right peaks are resonant photoemission peaks, and left peaks Auger contributions; in between they mix. Inset shows the XAS resonance. The decay spectra corresponding to the colored dots are represented with thicker lines. Bottom: 2D plot of the intensity of the complete set (shown in derivative mode in order to enhance the Auger contribution), indicating Auger peaks by variation of electron binding energy with photon energy (inclined lines in left part) and Raman peaks with constant binding energy (vertical lines at right; overlap in center).

The generally short CT times might appear surprising at first, considering the vanishing empty density of states (DOS) of Gr near the Dirac point. However, the Ar^{c+} 4s energies are in the range 1.2 to 2.7 eV above E_F (see the values in Table 1), i.e., in a range with considerable empty surface DOS on Gr, as will be discussed.

The main features of our findings are the large differences among the τ_{CT} values measured on Gr layers on the various supports. While there might be minor changes of the adsorption energy and site of Ar on the various Gr surfaces (which in fact we use to separate the contributions of L and H regions on Gr/Ru(0001), which may lead to (probably small) changes of the Ar–Gr distance), our results show an unexpectedly large dispersion of CT times in the various Gr situations, which cannot be explained by different Ar ground states. This is also corroborated by the equal behavior of the three decoupled cases: The Ar distance from graphene will depend on the overall van der Waals (vdW) attraction, to which Gr ML will contribute equally in all cases, but the different substrates will add differently due to their (different) densities and polarizabilities. The fact that these τ_{CT} values are the same

corroborates that ground-state effects are not important for CT. It also shows that there are no important influences of (certainly varying) defects in the layers or in the decoupling substrates, which have been shown to be important for scattering within the Gr layers.[22]

The large difference between the quasi-lifted off layers and the strongly coupled Gr/Ru situation would conform to the naïve expectation mentioned: that CT into a decoupled monolayer, a 2D final state, should be less efficient than that into a 3D system, in which fast, unimpeded spreading of the charge is possible in the substrate. However, for many other systems it was shown that the transfer to the first neighbor is decisive.[3–9] Furthermore, in the relevant energy range the empty DOS on freestanding Gr is quite high (see below), and even the decoupled 2D π^* layer is an extended system with very high carrier mobility in which the charge should also spread very quickly. It appears, then, that the comparatively slow CT to the essentially decoupled Gr layers must imply additional effects. We will therefore first examine the expected coupling considering the available information on the
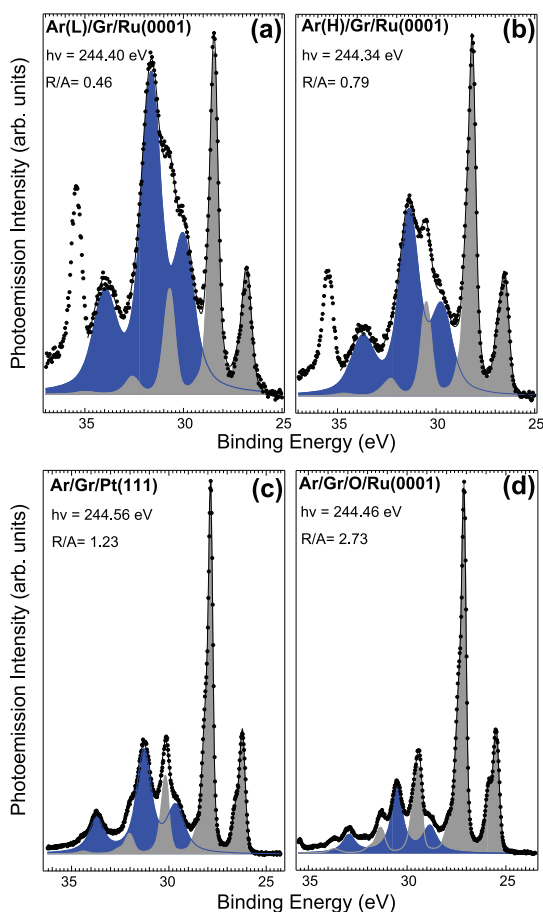
Figure 4. Measured decay spectra for excitation at the resonance energy (points) and their decomposition into Raman (gray shaded) and Auger (blue shaded) contributions obtained by the fitting procedure described in detail in ref 21, for the given Gr cases. The black lines between data points are the results of the fit. The ratio of the respective integrals yields the branching ratio into the Raman (core hole decay before CT) and Auger (CT before core hole decay) channels.

empty DOS of Gr in the relevant energy range (1.2 to 2.7 eV above E_F).

The equality of τ_{CT} on the three differently decoupled layers suggests that this constitutes the limiting case of CT to freestanding Gr. At first sight this equality might appear surprising since the energetic positions of the Ar^{c+} 4s state relative to E_F differ by more than 1 eV (Table 1). However, due to different (static) charge transfer and polarization of the Gr ML, the Dirac cone positions in the three cases differ by more than 1 eV as well (it lies at 0.45[12] to 0.42[14] eV *below* E_F for Gr/SiC, at ∼0.5 eV *above* E_F for Gr/O/Ru,[15] and has been calculated at ∼0.7 eV above E_F for Gr/SiO$_2$/Ru[23]). Relative to the electronic states of Gr the Ar^{c+} 4s state then lies at about the same position, at ∼2 eV above the Dirac point. At this energy there is considerable empty DOS derived from the π^* bands[24−28] to which the Ar^{c+} 4s level can couple. The high mobility in these bands then should let the transferred charge spread quickly. On this basis the measured CT time

appears unexpectedly long; a slowing-down effect must be operative. This probably stems from the final state character. In principle an atomically localized state can couple to states of any k-vector, provided they have sufficient density (DOS). In order to spread quickly, the Ar^{c+} 4s electron should be transferred to a laterally extended state. However, the mentioned area of high empty DOS lies between the K and M points,[26−28] *i.e.*, at high k values, while there are no states around the Γ point. Due to this and to the insulating character of the substrate, the transferred charge then is initially quite localized on the Gr. Then the transferred electron has to be scattered in order to spread in the π system. The overall process becomes a two-step process.[29] The transient local charge on the Gr before spreading can then lead to a slowdown of the transfer, somewhat similarly to effects observed in STM and termed dynamical Coulomb blockade,[30] effectively leading to partial reflection of the tunnelling charge and overall slowing-down. A thorough theoretical analysis would be highly desirable.

Next we discuss the large difference between these decoupled layers and the Gr/Ru cases, as well as the smaller but clear difference between the L and the H regions for Gr/Ru.[11,18,24,31−33] While considerable controversy still exists regarding the details of the periodically corrugated Gr ML on Ru(0001), there is agreement that in the "valleys" there is strong hybridization of Ru and Gr states. Essential agreement exists about the moiré rippling and its alignment between the Gr and the Ru surface meshes[11,17,18,24,31] in the H and L regions, but the distance between the two and its variation, the buckling Δh, are still controversial.

Experimental and theoretical values span between the extremes of Δh of 1.5[11,34] and 0.2 Å.[17] Early density functional theory (DFT) calculations have been influenced by neglect of the (certainly important) vdW contributions. Surface X-ray diffraction,[32] using the calculated Δh of 1.16 Å,[24] found the Ru surface to be antibuckled by 0.17 Å. A later low-energy electron diffraction study combined with DFT calculations[34] found a graphene corrugation of 1.5 Å. Recent DFT calculations including dispersion forces predict a value of 1.17[35] and 1.20 Å.[36]

Agreement exists that the Dirac cone is quenched in the valleys L. For the hills calculations predict its persistence,[18,24] suggesting pure vdW bonding, but no Dirac cone is found experimentally. The hills have been suggested to be molecule-like or quantum dot-like.[38] As to the valleys L, there is agreement that the opening of a gap indicates a rehybridization, which leads to doping of the Gr. This rehybridization has been assumed to occur with the Ru d_{z^2} orbitals, leading to a chemical bond Gr−Ru[37] or a metallic bond.[25]

The very short τ_{CT} for the valleys—only about twice the value for the bare Ru(0001) surface—supports this strong interaction between Gr and Ru states, leading to hybridized electronic states (d_z−p_z) for the aligned

geometry (half the C atoms are atop Ru atoms in the center of the valleys). The geometrical misfit leads to stretched C—C bonds and to gradual shifts from the (top-fcc) and (top-hcp) alignment within the super-structure unit cell, until the energy difference gets too large and the Gr layer lifts off.[35,37] So we expect strong coupling of the Ar^{c+} 4s electron to the C—Ru hybrids (which also have fitting symmetry) in the L and weak coupling in the H regions and direct delocalization of the transferred charge into the metal substrate. This qualitatively explains our results. However, if Gr in the H regions was essentially electronically decoupled from the substrate, CT rates there should be similar to those on the truly decoupled cases on SiC, O/Ru, and SiO_2/Ru. Also, if the H situation would be molecule-like or quantum dot-like, the charge should stay localized and CT should be slow. But we find the CT on the hills to be 3 times faster than on decoupled Gr and closer to the L regions. This could be taken as evidence of some Gr—Ru hybridization even in these regions. Alternatively, even without hybridization the tails of the Ru surface wave functions that exist between Gr and Ru could extend sufficiently above the Gr(H) surface. In fact on clean Ru it has been shown that monolayers of adsorbed atoms or molecules slow the CT from the Ar^{c+} 4s by factors of 2 or more.[6] The difference between L and H regions on Gr/Ru would then also be influenced by an increased tunnelling distance.

To further discuss the difference between valleys and hills on Gr/Ru(0001), we examine the literature, which indeed contains evidence from theory and experiments of the Gr—Ru interactions. Looking at the relevant energy range, several earlier calcula-tions and scanning tunnelling spectroscopy (STS) measurements[24,35,37,39] have found appreciable DOS at 0.5 to 2 eV above E_F, even though controversy exists about the assignment of peaks in this range.[40–42] In a calculation for Gr on Ru with varied distance[40] a Ru empty state mixing with Gr states has been found above 2 eV at Gr—Ru distances below 3 Å. A recent two-photon photoemission investigation of Gr/Ru[43] found well-defined surface states at 0.9 and ~2.5 eV above E_F, which were interpreted as due to states formed by hybridization of Ru with Gr empty states on H and L, respectively. The STS data cited show that there is considerable DOS below and above these resonances. Comparing to our results, which showed the Ar^{c+} 4s states at 1.2 eV (L) and 1.5 eV (H) above Fermi, we conclude that our donor states can couple into empty

DOS in both regions, even if they do not happen to match one of these surface resonances. Concluding this discussion, it appears that, as in STM, chemical (rehybridization) and distance effects are playing roles, and because they are connected and intertwined, they cannot be disentangled experimentally: The stronger coupling to the Gr—Ru hybrids in L is connected with the smaller distance between Gr and Ru so that the Ru DOS can reach through to above the surface more strongly. Theoretical treatments as done before for metal surfaces[8,9] will be needed to improve the under-standing and would benefit from our large database.

CONCLUSIONS

In conclusion, we have shown that charge transfer from resonantly excited adsorbed Ar atoms to the surfaces of Gr monolayers on various substrates is generally quite fast but varies widely for different Gr ML, leading to a variation of CT times up to a factor of almost 6. The CT rate is strongly accelerated by Gr coupling to the metallic substrates, which is caused by orbital mixing between empty metal states and Gr states in the relevant energy range. This has the consequence that transferred charge ends up directly in the 3D substrate. However, even for the cases that are usually considered to be bound only by vdW forces (Pt; hills on Ru) CT is much faster than on decoupled Gr. This may mean that even in these cases there is some hybridization or that there is an influence of distance as for decoupling atomic and molecular layers. Because of the connection between (chemical) coupling and dis-tance, these cannot be easily disentangled. For de-coupled monolayers, where the intrinsic states above the Gr surface are expected to determine the CT and the charge has to spread in 2D, the CT is much slower, even though the empty surface DOS is high at the Ar^{c+} 4s energy as well. We have discussed effects that could slow down the CT and its spreading in the quasi-freestanding Gr monolayer.

Our results are important for the overall understand-ing of the Gr electronic surface structure and the coupling of Gr MLs to their substrates. Extending the application of the CHC method to other adsorbates with different resonance energies on Gr ML should make it possible to determine the interaction between Gr and the underlying substrate in a wider energy range. Our present results are of potential importance for photonic applications of Gr, *e.g.*, for solar energy conversion, and for Gr contacts and electrochemistry.

METHODS

The differently coupled graphene monolayers have been prepared according to established procedures and character-ized by XPS (C 1s and relevant substrate peaks). All spectro-scopic measurements were done at the SuperESCA beamline of the synchrotron radiation source Elettra in Trieste/Italy. For Gr

on Ru(0001) and Pt(111) we used the well-documented pre-parations by thermal decomposition of ethene,[31,44] leading to Gr ML with moiré corrugation for Ru(0001), but flat Gr on Pt(111). Decoupling of a Gr/Ru layer by oxygen intercalation[15] was induced by prolonged oxygen exposure (~10^7 langmuir (L) (1 L = 10^{-6} Torr × s) with the sample at 450 K. Decoupling of a Gr

ML on Ru(0001) by a thin SiO$_2$ layer was accomplished by intercalating Si (about 5 ML) and subsequent oxidation as described in ref 16. A Gr/SiC[12,14] sample was kindly provided by Th. Seyller, Erlangen.[45] The layers were characterized by X-ray photoelectron spectroscopy (XPS) (C 1s, and relevant substrate core levels), and good agreement with previous measurements[46] was found.

Ar was adsorbed on Gr at 25 K; well-defined layers freed from remnants of multilayers were prepared by controlled heating monitored by fast XPS. The Ar layers for varied coverage were characterized by X-ray absorption (XAS) for the resonant Ar 2p$_{3/2}$→4s excitation, and Ar 2p$_{3/2}$ XPS by narrowband (∼40 meV) soft X-ray light. Since the XPS energies are referenced to the Fermi level, the differences of the XAS resonant photon energies of the Ar^{c+} 4s core excitons (where Ar^{c+} denotes the Ar atom with a core hole) and the corresponding XPS energies indicate the energetic position of the excited 4s level. Literature data for the position of the Dirac cone, E_D (where existing), can be used to relate the 4s position to the latter.

Decay spectra were recorded for closely spaced (every 20 meV) excitation energies throughout the Ar 2p$_{3/2}$→4s absorption resonances in all cases. All these sets have been analyzed in terms of τ_{CT} as usual[3,5,6] using their behavior with detuning the photon energy through the resonance peak, after subtraction of the small background. Due to some broadening of the Auger and spectator peaks, which was stronger for the former, three Auger peaks and four Raman peaks were fitted with equal spacings, lineshapes, and intensity ratios for all spectra of each set. The separated Auger and Raman contributions were then individually integrated and their ratios calculated. The CT values given here pertain to the resonance maxima. For detailed procedures see ref 21. The integrals I_R and I_A[3,5,6] were then used to calculate the CT time by multiplication with the Ar 2p$_{3/2}$ core hole lifetime (here assumed as 6 fs[47]), according to $\tau_{CT} = \tau_H I_R / I_A$. It is noteworthy that, as demonstrated in Figure 3, for all Gr monolayer surfaces the spectra were exceedingly well-defined and devoid of the background usually encountered on metal surfaces, even better resolved and cleaner than for the previous best case, H−Si(100).[21] This must be due to the low density of low-energy electron−hole excitations around E_F in Gr that could couple to the core hole decay processes. On metal surfaces the large background due to the high density of such coupled excitations can lead to ambiguities of analysis; this is not at all the case here.

Conflict of Interest: The authors declare no competing financial interest.

REFERENCES AND NOTES

1. Geim, A. K. Graphene: Status and Prospects. *Science* **2009**, *324*, 1530–1534.
2. Menzel, D. Electronically Induced Surface Chemistry: Localised Bond Breaking *versus* Delocalisation. *Surf. Interface Anal.* **2006**, *38*, 1702–1711.
3. Menzel, D. Ultrafast Charge Transfer at Surfaces Accessed by Core Electron Spectroscopies. *Chem. Soc. Rev.* **2008**, *37*, 2212–2223.
4. Föhlisch, A.; Feulner, P.; Hennies, F.; Fink, A.; Menzel, D.; Sanchez-Portal, D.; Echenique, P. M.; Wurth, W. Direct Observation of Electron Dynamics in the Attosecond Domain. *Nature* **2005**, *436*, 373–376.
5. Brühwiler, P. A.; Karis, O.; Mårtensson, N. Charge-Transfer Dynamics Studied Using Resonant Core Spectroscopies. *Rev. Mod. Phys.* **2002**, *74*, 703–740.
6. Wurth, W.; Menzel, D. Ultrafast Electron Dynamics at Surfaces Probed by Resonant Auger Spectroscopy. *Chem. Phys.* **2000**, *251*, 141–149.
7. Gel'mukhanov, F.; Ågren, H. Resonant X-ray Raman Scattering. *Phys. Rep.* **1999**, *312*, 87–330.
8. Sánchez-Portal, D.; Menzel, D.; Echenique, P. M. First-Principles Calculation of Charge Transfer at Surfaces: The Case of Core-Excited Ar*(2p$_{3/2}^{-1}$4s) on Ru(0001). *Phys. Rev. B* **2007**, *76*, 235406.
9. Vijayalakshmi, S.; Föhlisch, A.; Hennies, F.; A., P.; Nagasono, M.; Wurth, W.; Borisov, A.; Gauyacq, J. Surface Projected Electronic Band Structure and Adsorbate Charge Transfer Dynamics: Ar Adsorbed on Cu(111) and Cu(100). *Chem. Phys. Lett.* **2006**, *427*, 91–95.
10. Batzill, M. The Surface Science of Graphene: Metal Interfaces, CVD Synthesis, Nanoribbons, Chemical Modifications, and Defects. *Surf. Sci. Rep.* **2012**, *67*, 83–115.
11. Wintterlin, J.; Bocquet, M.-L. Graphene on Metal Surfaces. *Surf. Sci.* **2009**, *603*, 1841–1852.
12. Bostwick, A.; Ohta, T.; Seyller, T.; Horn, K.; Rotenberg, E. Quasiparticle Dynamics in Graphene. *Nat. Phys.* **2007**, *3*, 36–40.
13. Seyller, T.; Emtsev, K.; Gao, K.; Speck, F.; Ley, L.; Tadich, A.; Broekman, L.; Riley, J.; Leckey, R.; Rader, O.; et al. Structural and Electronic Properties of Graphite Layers Grown on SiC(0001). *Surf. Sci.* **2006**, *600*, 3906–3911.
14. Starke, U.; Riedl, C. Epitaxial Graphene on SiC(0001) and SiC(000$\bar{1}$): from Surface Reconstructions to Carbon Electronics. *J. Phys.: Condens. Matter* **2009**, *21*, 134016.
15. Sutter, P.; Sadowski, J. T.; Sutter, E. A. Chemistry under Cover: Tuning Metal-Graphene Interaction by Reactive Intercalation. *J. Am. Chem. Soc.* **2010**, *132*, 8175–8179.
16. Lizzit, S.; Larciprete, R.; Lacovig, P.; Dalmiglio, M.; Orlando, F.; Baraldi, A.; Gammelgaard, L.; Barreto, L.; Bianchi, M.; Perkins, E.; et al. Transfer-Free Electrical Insulation of Epitaxial Graphene from its Metal Substrate. *Nano Lett.* **2012**, *12*, 4503–4507.
17. Borca, B.; Barja, S.; Garnica, M.; Minniti, M.; Politano, A.; Rodriguez-Garca, J. M.; Hinarejos, J. J.; Faras, D.; de Parga, A. L. V.; Miranda, R. Electronic and Geometric Corrugation of Periodically Rippled, Self-Nanostructured Graphene Epitaxially Grown on Ru(0001). *New J. Phys.* **2010**, *12*, 093018.
18. Brugger, T.; Günther, S.; Wang, B.; Dil, J. H.; Bocquet, M.-L.; Osterwalder, J.; Wintterlin, J.; Greber, T. Comparison of Electronic Structure and Template Function of Single-Layer Graphene and a Hexagonal Boron Nitride Nanomesh on Ru(0001). *Phys. Rev. B* **2009**, *79*, 045407.
19. Keller, C.; Stichler, M.; Comelli, G.; Esch, F.; Lizzit, S.; Menzel, D.; Wurth, W. Femtosecond Dynamics of Adsorbate Charge-Transfer Processes as Probed by High-Resolution Core-Level Spectroscopy. *Phys. Rev. B* **1998**, *57*, 11951–11954.
20. Mårtensson, N.; Weinelt, M.; Karis, O.; Magnuson, M.; Wassdahl, N.; Nilsson, A.; Stöhr, J.; Samant, M. Coherent and Incoherent Processes in Resonant Photoemission. *Appl. Phys. A: Mater. Sci. Process.* **1997**, *65*, 159–167.
21. Lizzit, S.; Zampieri, G.; Kostov, K. L.; Tyuliev, G.; Larciprete, R.; Petaccia, L.; Naydenov, B.; Menzel, D. Charge Transfer from Core-Excited Argon Adsorbed on Clean and Hydrogenated Si(100): Ultrashort Timescales and Energetic Structure. *New J. Phys.* **2009**, *11*, 053005.
22. Farmer, D. B.; Perebeinos, V.; Lin, Y.-M.; Dimitrakopoulos, C.; Avouris, P. Charge Trapping and Scattering in Epitaxial Graphene. *Phys. Rev. B* **2011**, *84*, 205417.
23. Fan, X.; Zheng, W.; Chihaia, V.; Shen, Z.; Kuo, J.-L. Interaction between Graphene and the Surface of SiO$_2$. *J. Phys.: Condens. Matter* **2012**, *24*, 305004.
24. Wang, B.; Bocquet, M.-L.; Marchini, S.; Günther, S.; Wintterlin, J. Chemical Origin of a Graphene Moiré Overlayer on Ru(0001). *Phys. Chem. Chem. Phys.* **2008**, *10*, 3530–3534.
25. Peng, X.; Ahuja, R. Epitaxial Graphene Monolayer and Bilayers on Ru(0001): *Ab Initio* Calculations. *Phys. Rev. B* **2010**, *82*, 045425.
26. Silkin, V. M.; Zhao, J.; Guinea, F.; Chulkov, E. V.; Echenique, P. M.; Petek, H. Image Potential States in Graphene. *Phys. Rev. B* **2009**, *80*, 121408.

27. Kogan, E.; Nazarov, V. U. Symmetry Classification of Energy Bands in Graphene. *Phys. Rev. B* **2012**, *85*, 115418.

28. Voloshina, E.; Dedkov, Y. Graphene on Metallic Surfaces: Problems and Perspectives. *Phys. Chem. Chem. Phys.* **2012**, *14*, 13502–13514.

29. Moth-Poulsen, K.; Bjørnholm, T. Molecular Electronics with Single Molecules in Solid-State Devices. *Nat. Nanotechnol.* **209**, *4*, 551−556.

30. Brun, C.; Müller, K. H.; Hong, I.-P.; Patthey, F. m. c.; Flindt, C.; Schneider, W.-D. Dynamical Coulomb Blockade Observed in Nanosized Electrical Contacts. *Phys. Rev. Lett.* **2012**, *108*, 126802.

31. Marchini, S.; Günther, S.; Wintterlin, J. Scanning Tunneling Microscopy of Graphene on Ru(0001). *Phys. Rev. B* **2007**, *76*, 075429.

32. Martoccia, D.; Willmott, P. R.; Brugger, T.; Björck, M.; Günther, S.; Schlepütz, C. M.; Cervellino, A.; Pauli, S. A.; Patterson, B. D.; Marchini, S.; *et al*. Graphene on Ru(0001): A 25 × 25 Supercell. *Phys. Rev. Lett.* **2008**, *101*, 126102.

33. Martoccia, D.; Björck, M.; Schlepütz, C. M.; Brugger, T.; Pauli, S. A.; Patterson, B. D.; Greber, T.; Willmott, P. R. Graphene on Ru(0001): a Corrugated and Chiral Structure. *New J. Phys.* **2010**, *12*, 043028.

34. Moritz, W.; Wang, B.; Bocquet, M.-L.; Brugger, T.; Greber, T.; Wintterlin, J.; Günther, S. Structure Determination of the Coincidence Phase of Graphene on Ru(0001). *Phys. Rev. Lett.* **2010**, *104*, 136102.

35. Iannuzzi, M.; Hutter, J. Comparative Study of the Nature of Chemical Bonding of Corrugated Graphene on Ru(0001) and Rh(111) by Electronic Structure Calculations. *Surf. Sci.* **2011**, *605*, 1360–1368.

36. Stradi, D.; Barja, S.; Díaz, C.; Garnica, M.; Borca, B.; Hinarejos, J. J.; Sánchez-Portal, D.; Alcamí, M.; Arnau, A.; Vázquez de Parga, A. L.; *et al*. Role of Dispersion Forces in the Structure of Graphene Monolayers on Ru Surfaces. *Phys. Rev. Lett.* **2011**, *106*, 186102.

37. Wang, B.; Günther, S.; Wintterlin, J.; Bocquet, M.-L. Periodicity, Work Function and Reactivity of Graphene on Ru(0001) from First Principles. *New J. Phys.* **2010**, *12*, 043041.

38. Zhang, H. G.; Hu, H.; Pan, Y.; Mao, J. H.; Gao, M.; Guo, H. M.; Du, S. X.; Greber, T.; Gao, H.-J. Graphene Based Quantum Dots. *J. Phys.: Condens. Matter* **2010**, *22*, 302001.

39. Gyamfi, M.; Eelbo, T.; Waśniowska, M.; Wiesendanger, R. Inhomogeneous Electronic Properties of Monolayer Graphene on Ru(0001). *Phys. Rev. B* **2011**, *83*, 153418.

40. Borca, B.; Barja, S.; Garnica, M.; Sánchez-Portal, D.; Silkin, V. M.; Chulkov, E. V.; Hermanns, C. F.; Hinarejos, J. J.; Vázquez de Parga, A. L.; Arnau, A.; *et al*. Potential Energy Landscape for Hot Electrons in Periodically Nanostructured Graphene. *Phys. Rev. Lett.* **2010**, *105*, 036804.

41. Zhang, H. G.; Greber, T. Comment on "Potential Energy Landscape for Hot Electrons in Periodically Nanostructured Graphene". *Phys. Rev. Lett.* **2010**, *105*, 219701.

42. Borca, B.; Barja, S.; Garnica, M.; Sánchez-Portal, D.; Silkin, V. M.; Chulkov, E. V.; Hermanns, C. F.; Hinarejos, J. J.; Vázquez de Parga, A. L.; Arnau, A.; *et al*. Reply:. *Phys. Rev. Lett.* **2010**, *105*, 219702.

43. Armbrust, N.; Güdde, J.; Jakob, P.; Höfer, U. Time-Resolved Two-Photon Photoemission of Unoccupied Electronic States of Periodically Rippled Graphene on Ru(0001). *Phys. Rev. Lett.* **2012**, *108*, 056801.

44. Gao, M.; Pan, Y.; Huang, L.; Hu, H.; Zhang, L. Z.; Guo, H. M.; Du, S. X.; Gao, H.-J. Epitaxial Growth and Structural Property of Graphene on Pt(111). *Appl. Phys. Lett.* **2011**, *98*, 033101.

45. Emtsev, K. V.; Bostwick, A.; Horn, K.; Jobst, J.; Kellogg, G. L.; Ley, L.; McChesney, J. L.; Ohta, T.; Reshanov, S. A.; Rohrl, J.; *et al*. Towards Wafer-Size Graphene Layers by Atmospheric Pressure Graphitization of Silicon Carbide. *Nat. Mater.* **2009**, *8*, 203–207.

46. Preobrajenski, A. B.; Ng, M. L.; Vinogradov, A. S.; Mårtensson, N. Controlling Graphene Corrugation on Lattice-Mismatched Substrates. *Phys. Rev. B* **2008**, *78*, 073401.

47. Krause, M. O. Atomic Radiative and Radiationless Yields for K and L Shells. *J. Phys. Chem. Ref. Data* **1979**, *8*, 307–327.